Identification of intra-helical bifurcated H-bonds as a new type of gate in K^+ channel

Oliver Rauh[1], Martin Urban[2], Leonhard M. Henkes[2], Tobias Winterstein[1], Timo Greiner[1], James L. Van Etten[3], Anna Moroni[4], Stefan M. Kast[2], Gerhard Thiel[1*], Indra Schroeder[1]

[1]Plant Membrane Biophysics, Technical University Darmstadt, Darmstadt, Germany, [2]Physikalische Chemie III, Technische Universität Dortmund, Dortmund, Germany, [3]Department of Plant Pathology and Nebraska Center for Virology, University of Nebraska Lincoln, Lincoln, Nebraska, United States 68583-0900, [4]Department of Biosciences and CNR IBF-Mi, Università degli Studi di Milano, Milano, Italy

* Corresponding author E-mail: thiel@bio.tu-darmstadt.de

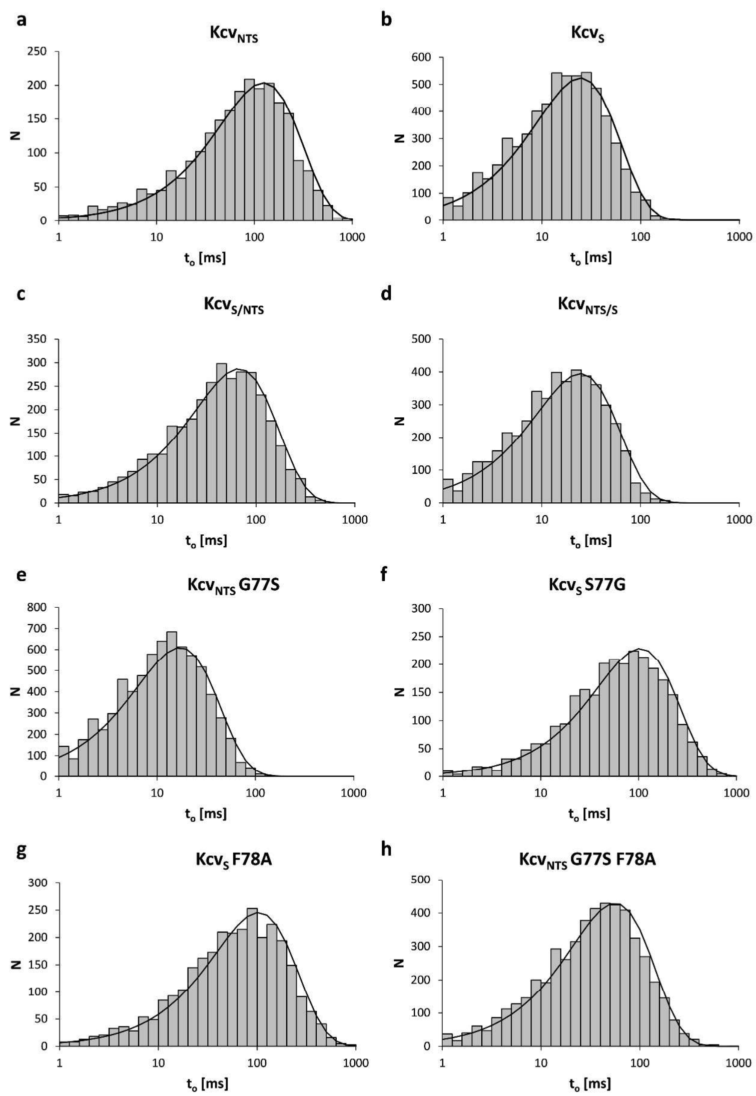

Supplementary Figure 1.

Open dwell times of Kcv channels

Dwell time histograms from recordings at +120 mV for Kcv_{NTS}, Kcv_S and chimeras/ mutants. All open dwell time histograms can be fitted with a single exponential.

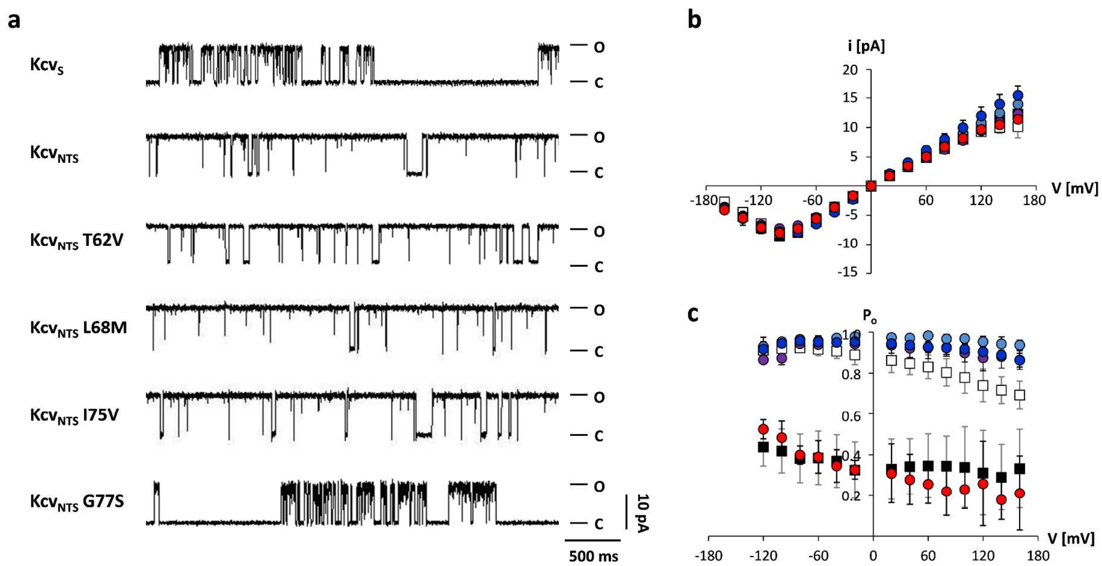

Supplementary Figure 2.

Only the exchange G77S in Kcv_{NTS} results in the electrophysiological phenotype of Kcv_S.

To identify the relevant AA in TMD2 for gating we mutated all 4 candidates in Kcv_{NTS} into the respective residue of Kcv_S. **(a)** Characteristic single channel fluctuations of the wt channels Kcv_S and Kcv_{NTS} as well as the Kcv_{NTS} mutants T62V, L68M, I75V and G77S at +120 mV in planar DPhPC bilayers. **(b)** Mean single channel i/V relations (± sd) and **(c)** mean open probabilities (± sd) of Kcv_{NTS} (open squares, n = 6), Kcv_S (filled squares, n = 9), Kcv_{NTS} T62V (purple circles, n = 4), Kcv_{NTS} L68M (light blue circles, n = 3), Kcv_{NTS} I75V (blue circles, n = 4) and Kcv_{NTS} G77S (red circles, n = 5).

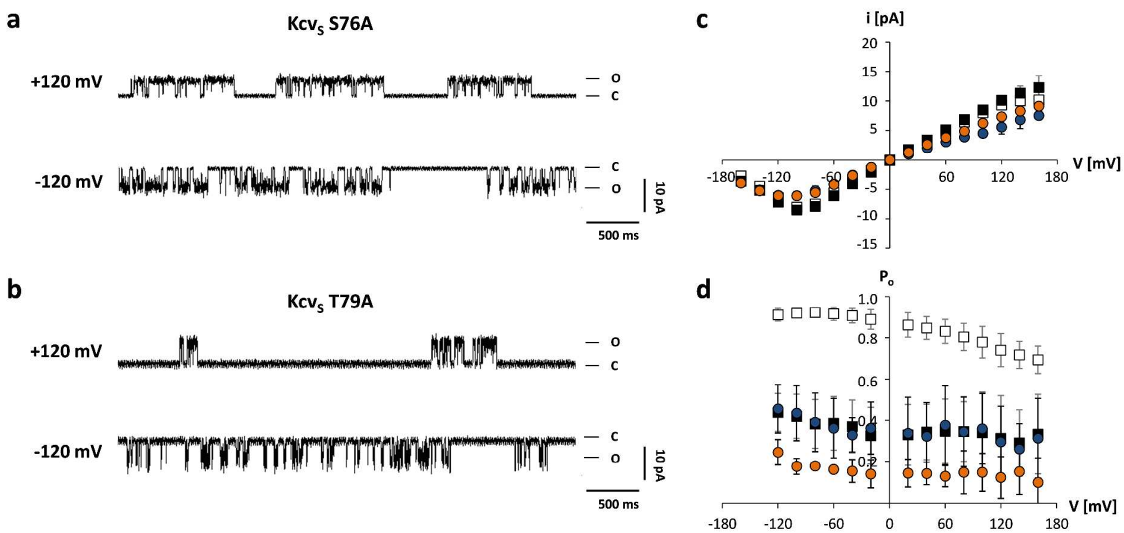

Supplementary Figure 3.

AAs S76 and T79 in Kcv$_S$ do not contribute to the long lived closed time.

Characteristic single channel fluctuations of mutant Kcv$_S$ S76A **(a)** and Kcv$_S$ T79A **(b)** at +/- 120 mV in planar lipid bilayers. **(c)** Mean single channel i/V relations (± sd) and **(d)** mean open probabilities (± sd) of Kcv$_{NTS}$ (open squares), Kcv$_S$ (filled squares), Kcv$_S$ T79A (orange circles, n = 4) and Kcv$_S$ S76A F78A (blue circles, n = 3).

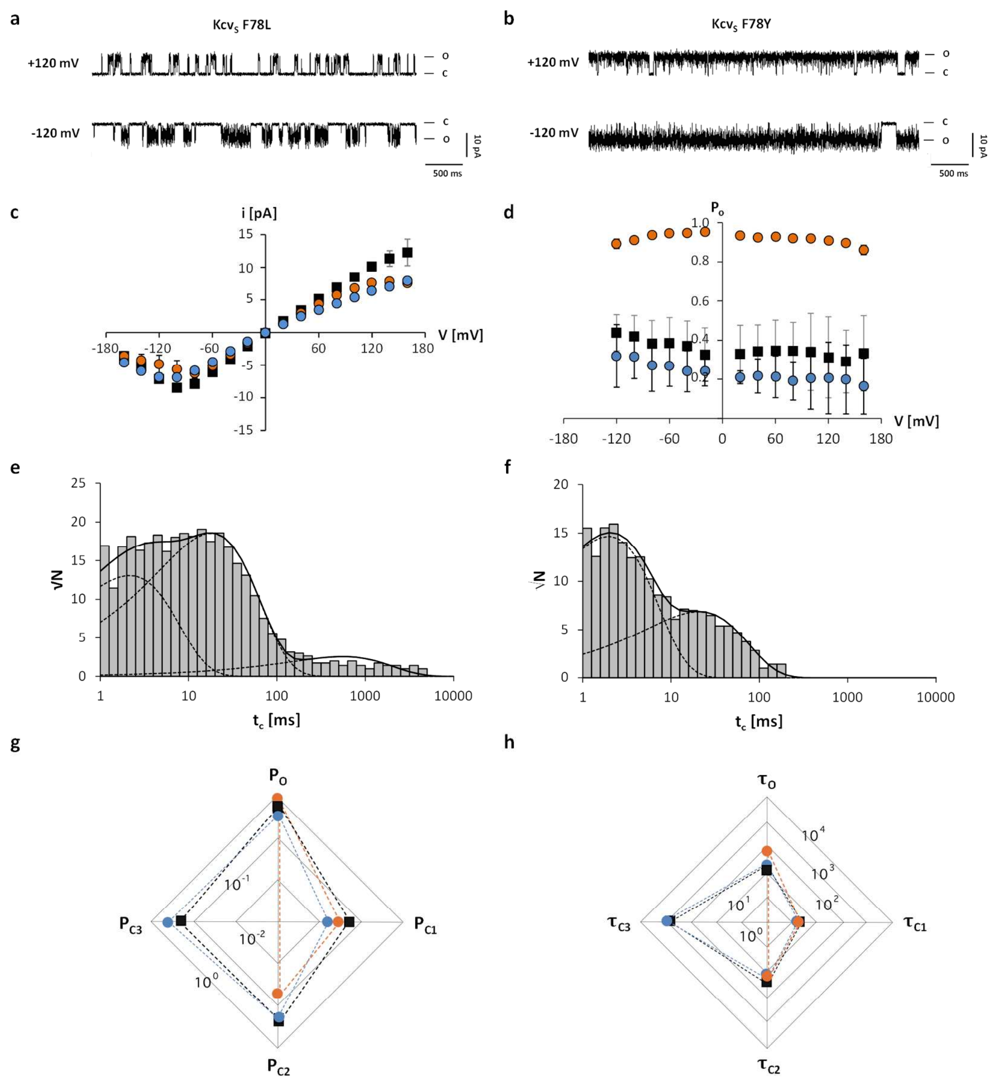

Supplementary Figure 4.

The gating function of the aromatic side chain of F78 can be substituted by the hydrophobic AA Leu but not by the aromatic side chain of Tyr.

Characteristic single channel fluctuations of mutant Kcv$_S$ F78L **(a)** and Kcv$_S$ F78Y **(b)** at +/- 120 mV in planar lipid bilayers. **(c)** Mean single channel i/V relations (± sd) and **(d)** mean open probabilities (± sd) of Kcv$_S$ (filled squares), Kcv$_S$ F78Y (orange circles, n = 3) and Kcv$_S$ F78L (blue circles, n = 3). Exemplary closed dwell times at +120 mV for Kcv$_S$ F78L **(e)** and Kcv$_S$ F78Y **(f)**. The data in **F** can be fitted with two exponentials while the data in **E** require a third exponential. **(g)** Probabilities (P) of the wt channel and mutants for occupying the open state (O) and the closed states (C1-C3) and mean lifetimes (in ms) of the open state (τ_o) and of the three closed states (τ_{c1}-τ_{c3}) **(h)**. The probabilities of occupancy and mean lifetimes were calculated from three independent 5 min recordings. The symbols in d, g and h correspond to those in c.

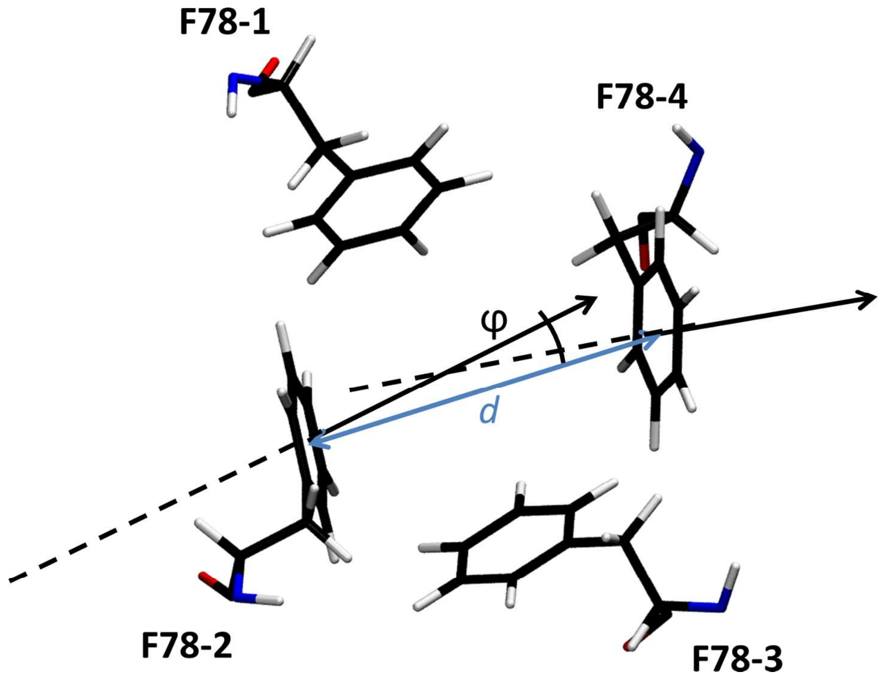

Supplementary Figure 5.

Definition of distance-angle pairs of F77 in Kcv_{NTS} and Kcv_S tetramers. The image illustrates the geometric criteria with distance *d* and angle φ for characterizing π-stack geometries in Fig. 7.

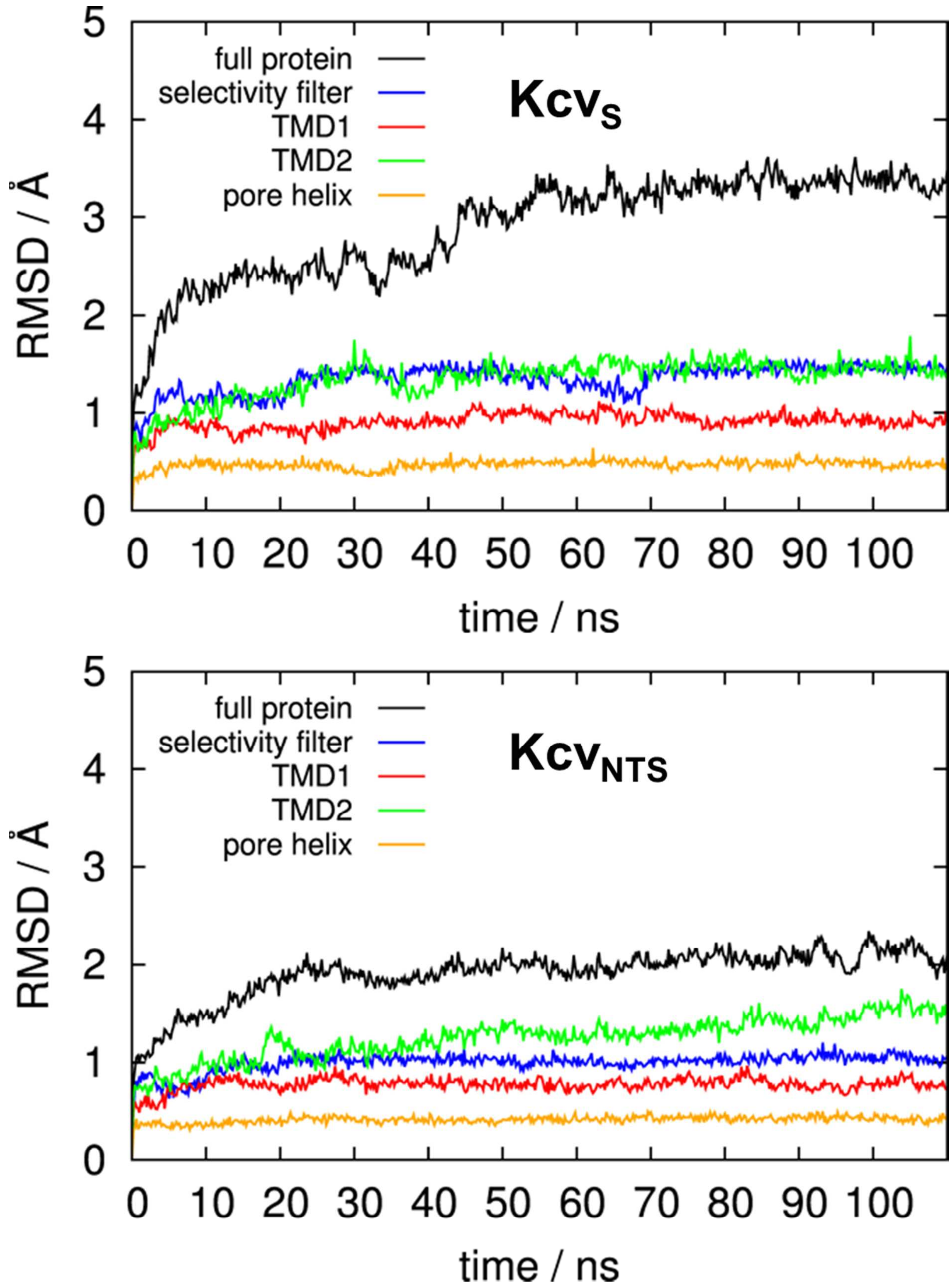

Supplementary Figure 6.

Demonstration of MD simulation stability for Kcv$_S$ (top) and Kcv$_{NTS}$ (bottom) models as measured by the root mean square deviations (RMSD) for various protein structure components with respect to the start of production runs.

	τ_o / ms	τ_{C1} / ms	τ_{C2} / ms	τ_{C3} / ms	P_O	P_{C1}	P_{C2}	P_{C3}
Kcv_{NTS}	79.1 ± 18.6	1.3 ± 0.2	24.0 ± 3.9	-	0.874 ± 0.073	0.008 ± 0.002	0.117 ± 0.075	0
Kcv_S	15.1 ± 2.5	1.8 ± 0.8	23.8 ± 9.4	480 ± 145	0.525 ± 0.101	0.047 ± 0.029	0.208 ± 0.095	0.220 ± 0.152
$Kcv_{S/NTS}$	63.5 ± 28.4	1.1 ± 0.5	47.6 ± 12.2	-	0.704 ± 0.171	0.008 ± 0.003	0.252 ± 0.171	0
$Kcv_{NTS/S}$	15.4 ± 6.4	2.1 ± 1.1	17.0 ± 3.4	1070 ± 118	0.227 ± 0.053	0.018 ± 0.011	0.109 ± 0.028	0.647 ± 0.028
Kcv_S S77G	79.7 ± 15.7	1.3 ± 0.1	28.4 ± 3.6	-	0.904 ± 0.029	0.012 ± 0.004	0.084 ± 0.031	0
Kcv_{NTS} G77S	11.2 ± 0.4	1.2 ± 0.2	15.1 ± 4.4	354 ± 220	0.540 ± 0.032	0.036 ± 0.007	0.245 ± 0.035	0.179 ± 0.074
Kcv_S F78A	42.1 ± 17.2	0.6 ± 0.1	7.9 ± 4.2	-	0.971 ± 0.014	0.014 ± 0.005	0.015 ± 0.017	0
Kcv_{NTS} G77S F78A	63.7 ± 60.1	1.3 ± 0.5	27.8 ± 16.5	-	0.926 ± 0.026	0.026 ± 0.010	0.051 ± 0.018	0
Kcv_S F78L	21.8 ± 13.9	1.7 ± 0.6	13.5 ± 5.0	983 ± 419	0.348 ± 0.126	0.017 ± 0.011	0.199 ± 0.171	0.436 ± 0.305
Kcv_S F78Y	56.4 ± 6.0	1.9 ± 0.2	16.9 ± 2.1	-	0.922 ± 0.012	0.025 ± 0.002	0.052 ± 0.013	0
Kcv_{NTS} F78L	108.8 ± 16.4	1.3 ± 0.2	27.3 ± 3.8	-	0.916 ± 0.024	0.008 ± 0.001	0.077 ± 0.024	0

Table S1: Mean lifetimes and probabilities of occupancy of Kcv_{NTS}, Kcv_S and some selected mutants. The probabilities of occupancy P (±sd) and mean lifetimes τ (±sd) of the open state O and the three closed states C1, C2 and C3 were calculated from three independent 5 min recordings at +120 mV.